REPORT DOCUMENTATION PAGE

AFRL-SR-AR-TR-07-0515

1. REPORT DATE *(DD-MM-YYYY)*	2. REPORT TYPE	3. DATES COVERED (From – To)
	Final Technical Report	1 April 2006 – 31 August 2007

4. TITLE AND SUBTITLE
Seed Effort Toward "Multiscale Theoretical and Experimental Investigation of the Role of Structural Features on Damage Tolerance and Creep"

5a. CONTRACT NUMBER

5b. GRANT NUMBER
FA9550-06-1-0232

5c. PROGRAM ELEMENT NUMBER

6. AUTHOR(S)
Professor Amit Ghosh

5d. PROJECT NUMBER

5e. TASK NUMBER

5f. WORK UNIT NUMBER

7. PERFORMING ORGANIZATION NAME(S) AND ADDRESS(ES
University of Michigan
3003 South State Street
Ann Arbor MI 48109-1274

8. PERFORMING ORGANIZATION REPORT NUMBER

9. SPONSORING/MONITORING AGENCY NAME(S) AND ADDRESS(ES)
USAF/AFRL
AFOSR
875 North Randolph Street
Arlington VA 22203
Brett Conner/NA

10. SPONSOR/MONITOR'S ACRONYM(S)
AFOSR

11. SPONSORING/MONITORING AGENCY REPORT NUMBER
N/A

12. DISTRIBUTION AVAILABILITY STATEMENT

Distribution Statement A: Approved for public release. Distribution is unlimited.

13. SUPPLEMENTARY NOTES

14. ABSTRACT

This report summarizes research ideas and some results in relation to effort conducted toward understanding the role of grain boundaries and grain boundary defects on the mechanical properties of metals, and with evolving interest in testing and learning the behavior of small specimens. It has been shown that by considering grain boundaries having different properties from grains, strengthening of metals as affected by grain size can be predicted. The analysis reveals that deformation in polycrystalline metals is heterogeneous and strain concentration evolves near grain boundary triple points and defects present on the grain boundary. An apparatus has been developed to perform tensile tests on small size samples within the chamber of the SEM. The tested samples of Ti-1100 alloy show considerably greater rate of strain hardening than specimens that are of conventional size. Because the grain size of these samples are the same, the higher hardening rate is believed to be a result of interaction of slip with specimen surface which occurs to a great extent per unit volume in the small size samples. Unfortunately, this seed effort remained as a seed effort and we were unable to continue the planned work due to inavailability of funds.

15. SUBJECT TERMS

16. SECURITY CLASSIFICATION OF:	17. LIMITATION OF ABSTRACT	18. NUMBER OF PAGES	19a. NAME OF RESPONSIBLE PERSON
		30	

AFOSR Final Report

SEED EFFORT TOWARD "MULTISCALE THEORETICAL AND EXPERIMENTAL INVESTIGATION OF THE ROLE OF STRUCTURAL FEATURES ON DAMAGE TOLERANCE AND CREEP"

Contract No. FA9550-06-01-~~232~~ 0232

P.I. Amit Ghosh, University of Michigan
Graduate Student: Rick Lee

November 2007

Abstract

This report summarizes research ideas and some results in relation to effort conducted toward understanding the role of grain boundaries and grain boundary defects on the mechanical properties of metals, and with evolving interest in testing and learning the behavior of small specimens. It has been shown that by considering grain boundaries having different properties from grains, strengthening of metals as affected by grain size can be predicted. The analysis reveals that deformation in polycrystalline metals is heterogeneous and strain concentration evolves near grain boundary triple points and defects present on the grain boundary. An apparatus has been developed to perform tensile tests on small size samples within the chamber of the SEM. The tested samples of Ti-1100 alloy show considerably greater rate of strain hardening than specimens that are of conventional size. Because the grain size of these samples are the same, the higher hardening rate is believed to be a result of interaction of slip with specimen surface which occurs to a great extent per unit volume in the small size samples. Unfortunately, this seed effort remained as a seed effort and we were unable to continue the planned work due to inavailability of funds.

SEED EFFORT TOWARD "MULTISCALE THEORETICAL AND EXPERIMENTAL INVESTIGATION OF THE ROLE OF STRUCTURAL FEATURES ON DAMAGE TOLERANCE AND CREEP"

Contract No. FA9550-06-01-232; Initially Funded at $30,102

Participants:
P.I. Amit Ghosh, University of Michigan
Graduate Student: Rick Lee

AFOSR Managers: Brett Conner, Jay Tiley
Cognizant AFRL Scientists: S.L. Semiatin, J. Larsen

Motivation for Research

•Understanding Structure-Property Relations and Damage Development in Complex Multiphase Aerospace Alloys is far from complete

•This AFOSR Review Program attests to this fact

•Satisfactory Predictability of Mechanical Behavior of complex microstructures such as in Titanium alloys, quantifying grain size effect, sample size effect and local deformation effects require judiciously coupled theoretical and experimental studies

•Titanium Alloys in various heat treatment conditions have interfaces between crystallographically anisotropic and geometrically anisotropic phases, i.e. Relative to load axis, lamellae orientations change from one location to another, geometry of α–β interfaces change from one location to another.

Understanding of Damage Evolution in Creep and Fatigue remain largely empirical, or modeled in a statistical manner

Though damage is known to be influenced by microstructure, predictive modeling techniques have not considered evolution equations based on microstructure or phases

Grain boundary and phase boundary produce incompatibility of strain locally and the role of "geometrically necessary dislocations at grain boundaries are discussed but not incorporated into quantitative analysis

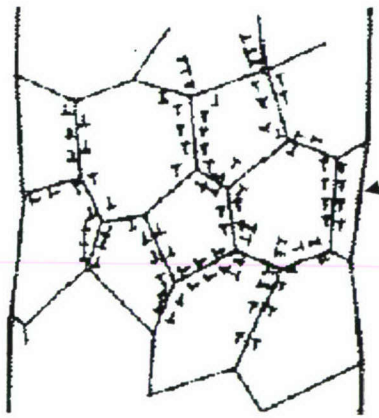

Every boundary cannot have equal density of GNDs

Microstructurally-based Understanding of Damage Requires Critical Analysis of what seems to be known

CSL Network Model of grain boundary claims regions of periodic lattice separated by disordered regions, but such models assume that grain boundary must be planar, but is it really planar?

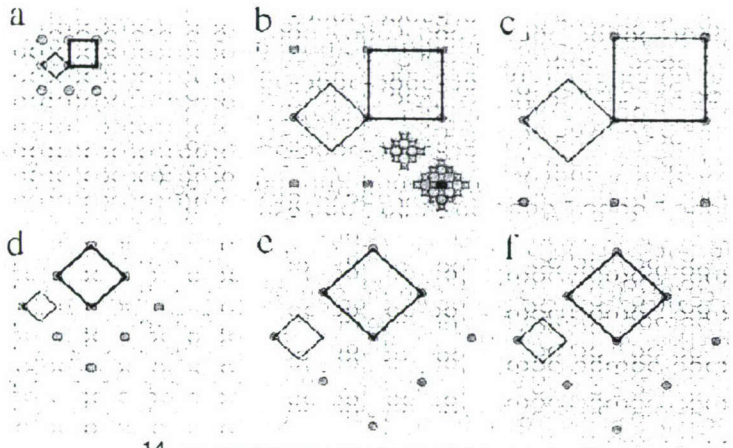

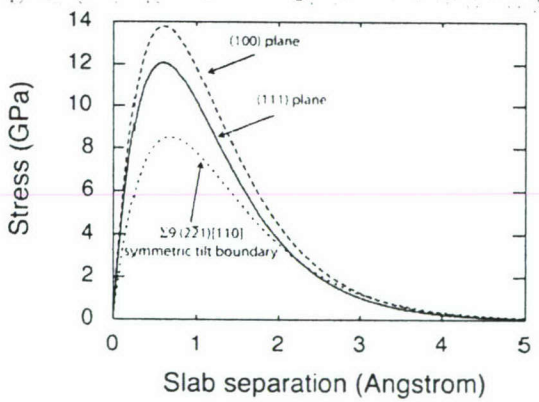

First-principles calculated traction curves for decohesion between (100) planes, (111) planes and of a Σ9, symmetric tilt boundary in fcc aluminum (Coutesy: Anton Van der Ven)

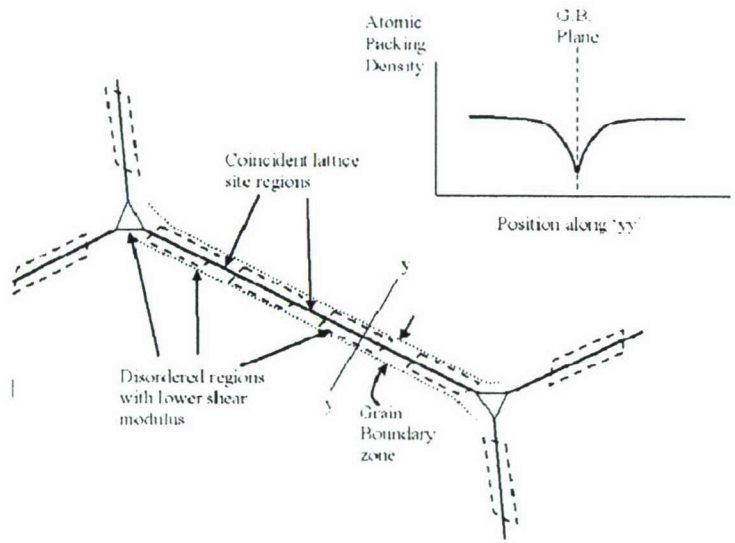

Atom density along boundary plane is lower, i.e. G is lower

Compliance must fluctuate along grain boundary causing local strain concentration in regions of disorder

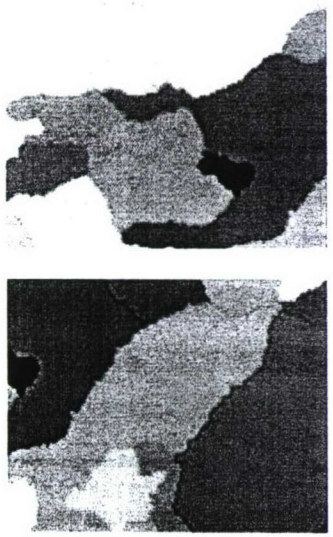

EBSD Images-
Groeber, Ghosh - OSU

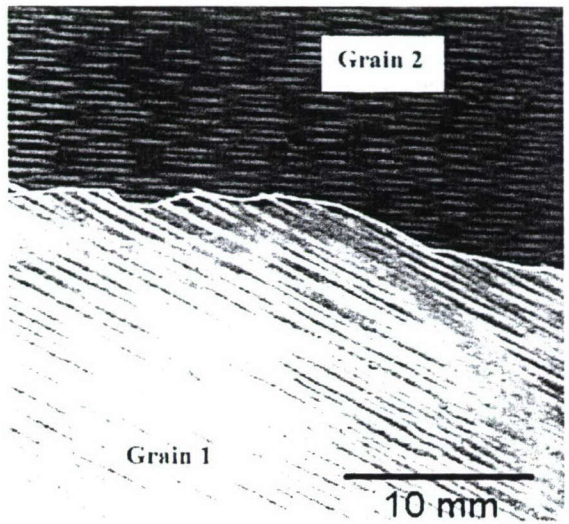

Grain boundary in a Cast Ni-base Superalloy – Li and Ghosh, U. Mich.

Evidence of Curvature and Protrusion on grain boundaries in length scales from nanometrer scale to centimeter scale

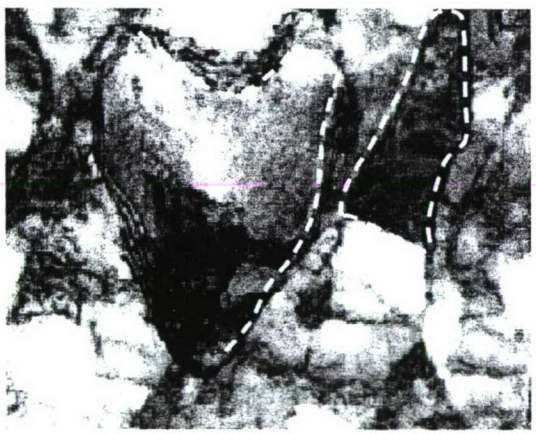

H. Maier et al.
UFG Fe

200 nm

Ghosh, Materials Science Forum

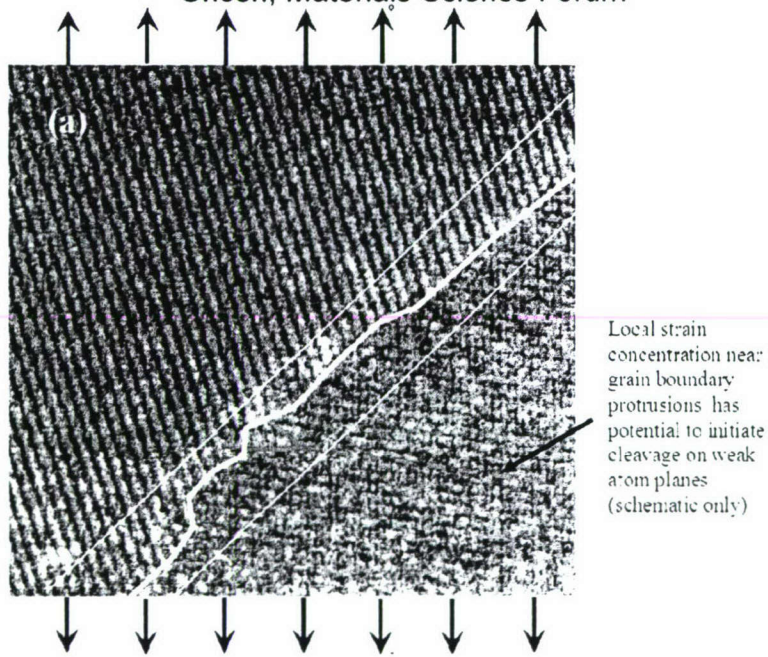

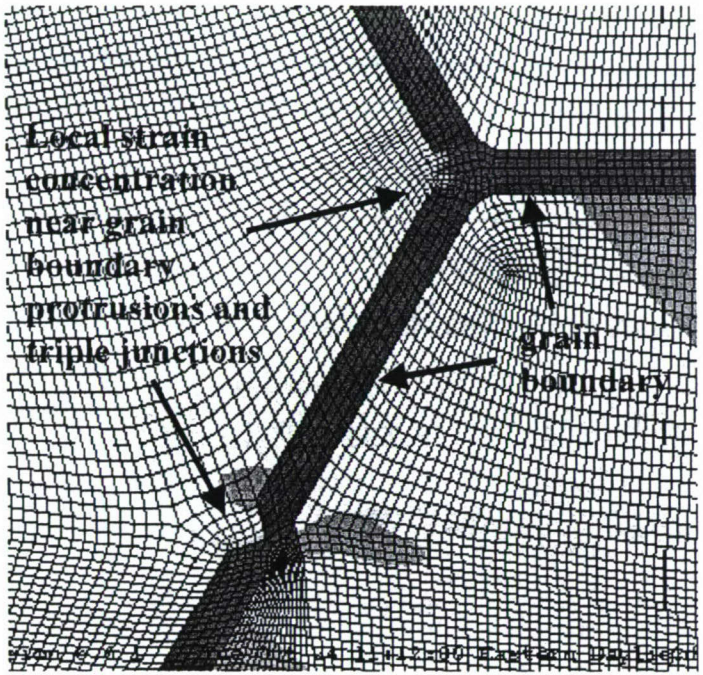

Simulation considers grain boundary as a separate cohesive phase of high dislocation density, with protrusions in it as in the actual microstructure

Strain concentration develops at grain boundary defects, and at locations of high local curvature, e.g. triple points

Experiments show those regions have high dislocation density

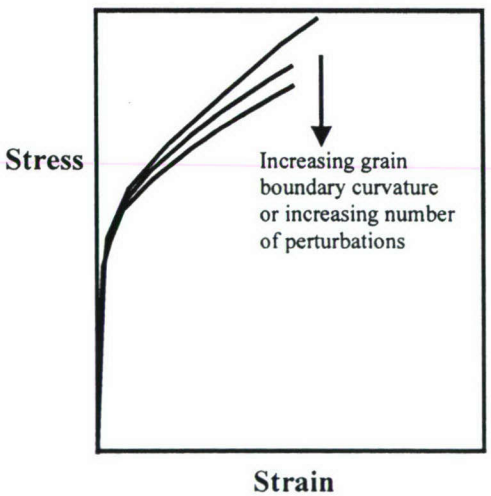

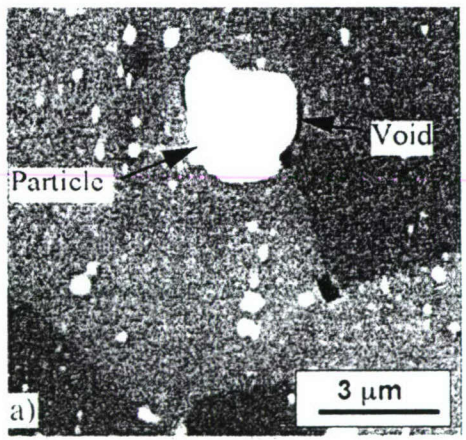

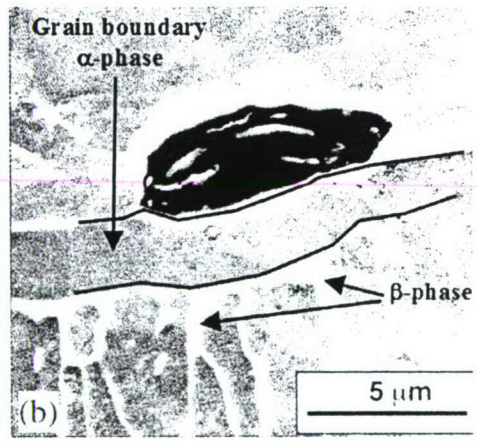

Predictive Simulation of deformation is planned on the basis of the following inputs

(1) Dislocation theory to guide grain boundary behavior

(2) Microscopic Tensile tests on single crystals taken from large grain polycrystals for grain matrix behavior

(3) EBSD to determine orientation and Taylor Factor

(4) Grain boundary geometry to simulate realistic defects

Experimental Plan would involve

Performing tensile test within the SEM to

(a) determine stress-strain relations

(b) characterize damage evolution

(c) local strain measurement

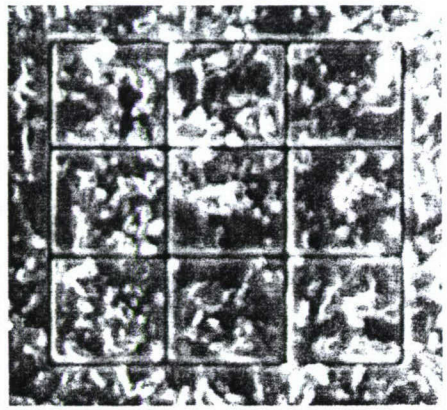

FIB machined sample with grid pattern etched with FIB

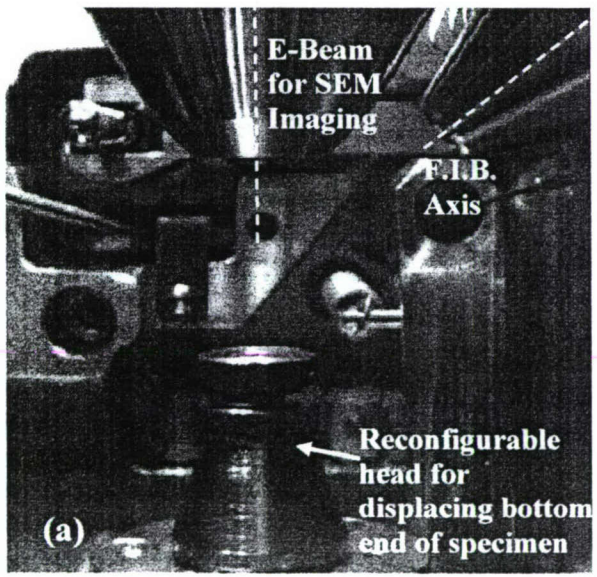

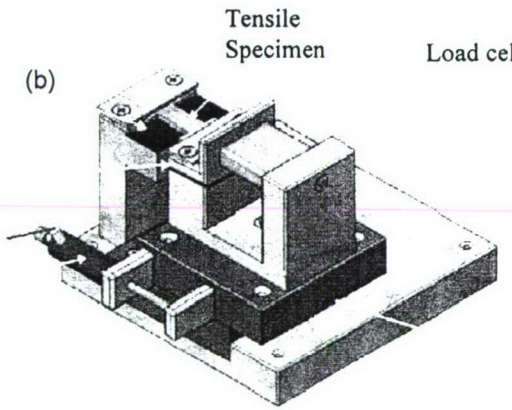

20 N load capacity

Figure (a) shows the inside view of SEM chamber, with viewing beam axis and FIB axis; (b) Fabricated sliding stage for controlled rate tensile and fatigue test of specimen, with provision for testing at elevated temperature (up to 400°C), being fabricated at this time

Samples for microscopic tests
from coarse grain thin foils

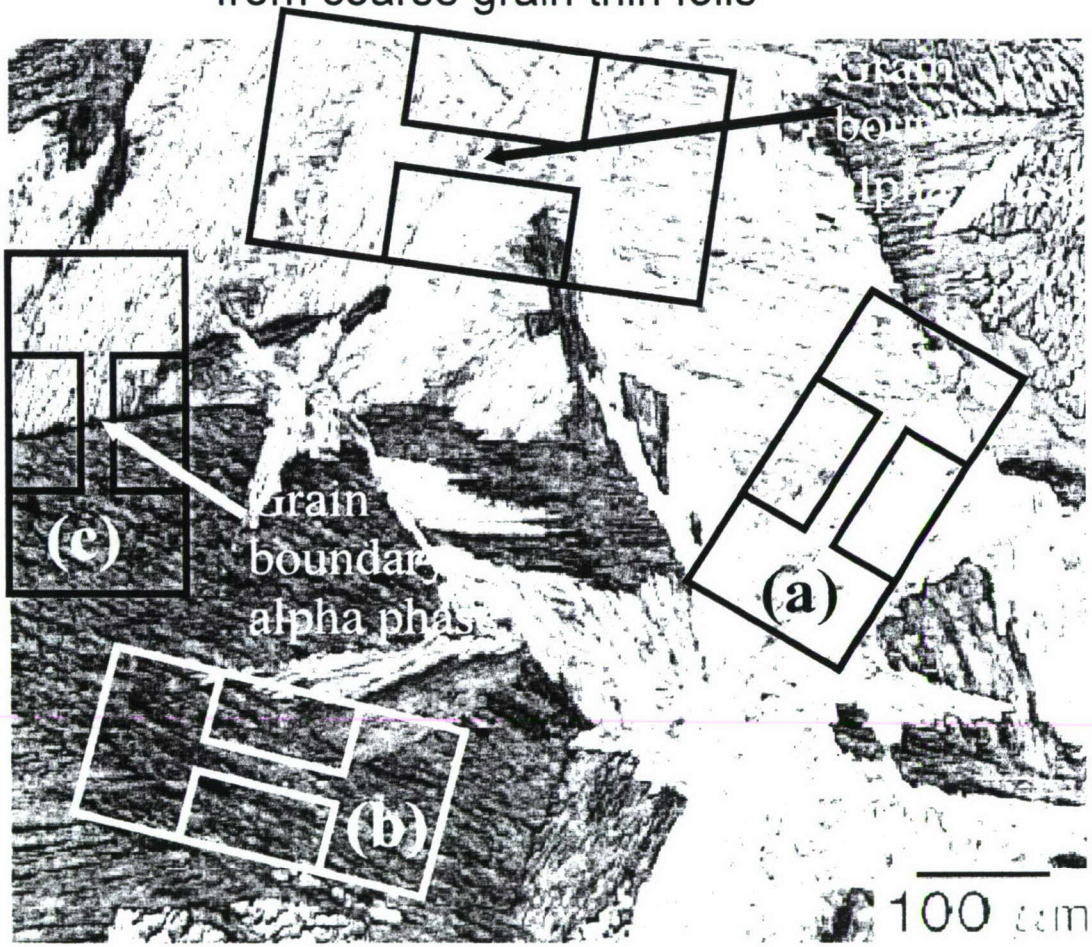

Introduction

Small sample test has gained increasing interest to researchers in the thin film area for their change of mechanical behaviors in the micron or nano-scale tests. Unlike regular tensile test, due to its miniature size small sample test usually requires a special test apparatus. Haque *et al* [1] performed the micro-tensile tests inside the SEM chamber on the 200nm thick, 23.5μm wide and 185μm long sputter deposited aluminum samples The load was applied by a piezo-actuator and strain measurement was done by measuring the amount of strain of the force sensor beam which directly connected to the aluminum specimen. Greek *et al* [2] tested the polysilicon films with different thickness of 10 μm and 2 μm thick, 10 μm wide and 1000μm long under the SEM. The load was applied and measured by the piezoelectric actuator and load sensor. Ruud and Josell [3] tested the Cu, Ag and Ni thin films of 1 cm long, 3.3 μm wide and 1.9-2.6μm thick in gauge area with the motor driven micrometer and load cell. Several other thin film tests were done on the different test apparatus [4-6]. These thin film researchers gave us many insights of material properties under the micron- scales and some interesting phenomenon were uncovered. The mechanical properties of the thin films usually differ from the bulk materials [1,2,6,10]. Yield strength of 33 times compared to the bulk material in the thin film aluminum was reported by Haque *et al*[1] and yield strength one tenth of the bulk value was found in the polysilicon thin film by Greek *et al* [2]. These deviations in mechanical properties from the bulk materials were believed to be caused by one or more of the following factors:

-thin film texture effect:

Strong texture was usually built when the thin film was deposited on the substrate and the orientation of the texture often time affected the measured strength value [4,10].

-grain size effect:

The grain size of the thin film usually can't exceed film's thickness and thus it's very dependant on the thickness of the film. $d^{-1/2}$ related Hall-Petch effect was well followed down to a certain range of the grain size[14-16]. However, the Hall-petch relation can't hold when the grain size reaches very small scale in nano-scaled thin films, the breakdown of the Hall-Petch effect were reported by several researchers [9-12].

-intrinsic stress

The deposited thin films often exhibit high intrinsic stress [13] and by which affected the strength value of the thin films.

-dislocation impingement of the thin film surface.

The surface of the film is considered obstacle for the advancing of the dislocations due to oxidation layer and/or rigid adjacent substrate. The dislocation impinged at the surface may cause the dislocation pile-ups and further increase the strength of the material.

-surface wrinkle/taut/slack/roughness of the thin film.

Wrinkles/slack/roughness usually found in the thin films, especially the free standing samples may be caused by inappropriate gripping and sometimes could impose errors in strain measurement [2, 3, 4].

Strengthening/softening of the materials in micron-level thin film tests is governed by more than one of the above mechanisms and hence it is not easy to determine the magnitude of the individual mechanism which attributed to the total change of the property of the micron-scale material. In this study we studied a new approach to investigate the micron-level material properties; Tensile test of micron-level small samples by using *in-situ* computer controlled test apparatus. Micron-scale small tensile samples were directly machined from the bulk material and hence we can rule out

-grain size effect that is inherent in deposited thin films

All the samples were from the same bulk so no change in grain sizes

-pre-formed texture

no texture was developed in the polycrystalline bulk material

-intrinsic stress

Little or no residual stress was built during the machining of the small samples.

-surface wrinkle/taut/slack

No bending/wrinkle/slack was found on the small samples prior to the test.

so that we can focus on the remaining strengthening/softening factors such as dislocation strengthening, surface strength and grain boundary effects.

Experiment

A 0.1mm thick Ti-1100 sheet was used in annealed condition as the base material for all the tensile samples that were tested in this study. The chemical composition of the Ti sheet is tabulated in Table 1.

Large sample test

The tensile test was first conducted on a large sample machined from the Ti-1100 sheet with 15mm long and 3mm wide in gauge section. A 4505 Instron frame was employed for the test and the strain rate was set at 0.5mm/min. Fig 1 shows a comparison between tested sample and untested sample and their stress-strain curve of the test is shown in Fig 2. The stress at failure of the large sample was measured by dividing the load before failure by the final cross-section area of the sample. The original sample failed at an overall strain of 0.1 represented by the dotted line in Fig 2. This is not the true strain at fracture. True strain at fracture was measured within the non-uniform strained region in the necked area. An extrapolation of the stress-strain was made which connected the original stress-strain curve to the fracture point. Some strain softening was seen in the extrapolation. The tensile strength of the large sample is around 1000MPa and the tensile elongation (engineering strain) measured from the gauge section is about 9.3%.

Small sample preparation

Compared to the tensile test conducted on the large sample, several small samples were made for the micro-scale tensile test. The small samples were prepared by cutting a 30

mm x 10 mm x 0.1mm rectangular piece from the Ti-1100 sheet and machined by abrasive micro-saw to create a multi-finger dumbbell configuration piece with three 0.150 mm x 5 mm x 0.1mm fingers in the middle and two 0.5 mm x 5 mm x 0.1mm supportive arms on each side. A photo of the small sample is shown in Fig 3. The supportive arms serve as a safety mechanism to protect the flimsy test fingers while samples are transported. The supportive arms would be cut open before starting the tensile test. To create a test gauge section, a combination of chemical etching method and Focused Ion Beam (FIB) etching was used. HF solution (10ml HF, 90ml ethyl alcohol) was used to locally etch the fingers of the machined samples to reduce the width down to 100μm. A subsequent sanding on the fingers would further bring down the thickness of the fingers from 100μm to around 30μm. Mechanical polishing on the top and bottom surfaces of the fingers would later be performed by using the 6μm colloidal silica. Although the top and bottom faces of the fingers could be mechanical polished, the vertical edges between the fingers still remained rough after previous mechanical machining and chemical etching, and might cause crack initiation or force concentration which could seriously affect the test results. To resolve this problem, as shown in Fig 4a, a 100 μm x 30 μm rectangular block on each side of the fingers were removed by focused ion beam(FIB) using the QUANTA 3D SEM . Four square grids were also etched on the surface of the finger to measure the strain during the pulling of test sample. As can be seen in Fig 4b, the FIB trimmed edge is clean and smooth compared to the untrimmed area, which allows measurement of test cross-section and to perform a more accurate micro-tensile test.

Mechanical system

A tensile test apparatus was specially designed to test the small samples. The design of this equipment was made by a fellow graduate student, Bilal Mansoor. Fig 5 shows the apparatus used for the micro tensile test. A computer controlled open-loop New Scale Technology Squiggle linear actuator (H) was used to apply constant crosshead speed to the loading section (G) of the test apparatus, and the load was transmitted through the slide stage (E) and mobile crosshead (B) to the small sample(C). The loads registered on the small sample were sensed by a Futek 5lbs load cell (D). The voltage output from load cell was originally calibrated and then recorded by a computer via a DAQ board and later translated back to the corresponding load values. The whole sets of the micro tensile apparatus were vacuum proved so that it can be set up inside the SEM chamber, which allowed the test process to be monitored by the SEM.

Tensile tests

Two preliminary tensile tests were conducted on one four-finger sample (sample 1) and one three-finger small sample (sample 2) outside the SEM chamber. Fig 6 showed the SEM picture of sample 1 before and after the test. The load-time value of the test is shown in Fig 7. The supportive arms of the small samples were cut open with a diamond saw before loading onto the test apparatus. The crosshead speed of the test apparatus was controlled by the open loop Squiggle linear actuator with resolution of 1μm/s. Load cell was calibrated before each test and load-time data was stored in the computer for the later use.

The samples were pulled all the way to failure with crosshead speed of 4μm/s. SEM photos of the before/after tests were taken on the samples for the strain measurement.

Another In-situ tensile test was conducted on a three-finger small sample (sample 3) inside the Quanta 200 3D FIB/SEM chamber, the test fingers of the sample was shown in Fig 8. The test was sectioned into 5 steps and the load-time values of each step was recorded and showed in Fig 9. The actuator stopped at the end of each step and a SEM photo was taken on the fingers before the next step begins. The initial crosshead speed was 1μm/s.In step 2 the actuator was reversed till the load dropped to zero and a higher crosshead speed of 4μm/s was applied. In step 5 the actuator was reversed again. The load dropped to 0.4N before a higher crosshead speed of 11μm/s was applied. The SEM photos taken at the end of each step were compared in Fig 10.

Test result and discussion

In the Fig 6 (b), we could see that after sample failed, three fingers (finger A,B,C) were further away from their counter parts than the fourth finger(finger D) which indicated that three fingers failed before the fourth one. The two load peaks on the load-time curve shown in Fig 7 also suggested the two-steps failure of the sample. Based on these investigations, we can assume that three fingers (finger A, B, C) broke at the first peak (peak 1) and followed by the breaking of finger D at the second peak (peak2). Before the first breaking (peak1), all four fingers were sharing the load. The final cross-sections of each finger were measure by the SEM photo taken at the fracture surface as shown in Fig 11. The stress at peak1 was calculated by dividing the load (9.4N) by the final cross-

sections of all four fingers (8601μm^2) and the strain was calculated by the following equation:

$$\varepsilon = \ln(\frac{A_0}{A_f})$$

where A_0 is the original cross-section and A_f is the final cross-section of the fingers.

The stress-strain value acquired from peak1 of the sample 1 was represented by point 1 in Fig 12. The stress-strain values before each failure happened on the sample 2 were also measure by the same method and were represented by point 2, 3 and 4 in Fig 12. The stress-strain curve of the large sample was also put into the figure as a base plot. For the In-situ test done on sample 3, not only the stress-strain value before failure could be measured from the post-test SEM photos, but the stress-strain values in each step of the test could also be determined by the In-situ observation. However, by observing the grids on the test fingers of sample 3 as shown in Fig 10, no strain was found till the sample was pulled to step 5; the load went up to 7.8N and by the in-situ SEM observation, two fingers (I and II) failed right after the load reaching that peak. Stress-strain value at the peak of step5 was measured and represented by point 5 in Fig 12. The dotted lines in Fig 12 showed the extrapolation of the stress-strain curve of the small samples and point 6 is the stress-strain value of the large sample right before the failure. Compared to the large sample test, extensive strain-hardening was found in the small sample tests. Table 2 listed the corresponding" average load-carrying areas "of each stress-strain points in Fig 12. The "average load carrying areas" was defined to be the average cross-section areas of the fingers which carried the load of the sample. It is found that with larger load carrying areas in the test sample such as point 6, the stress it carried is smaller than the load carried by the samples with smaller load carrying areas. The stress- area relationship in

between individual small samples was still undetermined. However, it is safe to say that much higher stress was carried by the small samples comparing to the large sample. This finding agrees with the test results of several previous researchers [1, 6, and 10], by which they found tensile tests done on the aluminum thin films showed a higher stress value than the bulk material. This may be explained by the increase in surface areas of the small samples. The surface area is served as a barrier for the advancing of the dislocations. As the samples become smaller, the fraction of surface area to total volume becomes larger and the strain hardening by the dislocation pile-ups on the surface becomes more and more prominent such that much higher stress values could be found in small samples than the large sample. However, this hardening effect weren't followed well in between small samples. Some comparatively larger small samples (larger average load carrying areas) have higher stress value and some smaller small samples (smaller average load carrying areas) have lower stress value as can be seen on the Fig 12 and Table 2. The hardening effect caused by the dislocation pile-ups at the surface could only give us an overall trend of the micron-level property change of the material. Some other deformation mechanisms of the micron-level material could exist and need to be studied.

Conclusions

Small samples around 100 μm wide, 30μm thick and 100 μm were successfully made from bulk material by series of cutting, chemical etching and focused ion beam trimming. *In-situ* tensile test was conducted inside the SEM chamber and higher flow stresses of the small samples were witnessed.

-Micron-level small samples can be machined from the bulk materials via precise machining and chemical etching.

- *In-situ* tensile test of the small samples can be conducted under SEM with the special designed test apparatus.

-Surface roughness of the small samples can be removed by the FIB machining and the test errors can be minimized.

-Higher flow stresses and strain hardening rate of the small samples compared with the large samples were observed. The fact that the rate of strain hardening increased indicates that the results are not due to FIB machining but increasing interaction of slip with the specimen surface.

-The strengthening of the small samples may be caused by the increasing in fraction of surface area to total volume, which shows considerable interaction of slip steps with sample surface.

-More detailed SEM or TEM study is needed to investigate and verify the deformation mechanism of the micron-level small samples.

Acknowledgments

Portions of this report and time for student advising were supported by other funds, but the authors are encouraged and intellectually stimulated to study the behaviors of these materials, and believe that this type of work should be continued.

References

[1] M.A Haque and M.T.A Saif," In-situ Tensile Testing of Nano-Scale Specimens in SEM and TEM". *Experimental Mechanics*, v 42, n 1, March 2002, p 123-8

[2] S. Greek, F. Ericson, S. Johansson and J. A.Schweitz. "In situ tensile strength measurements of thick-film and thin-film micromachined structures" *International Conference on Solid-State Sensors and Actuators, Proceedings*, v 2, 1995, p 56-59

[3] J.A Ruud, D. Josell and Spaepen. "A new method for tensile testing of thin films".

[4] Huang, H and Spaepen. "Tensile testing of free-standing Cu, Ag and Al thin films and Ag/Cu multilayers" *Acta Materialia* v 48 3261-3269 (2000)

[5] Yuan, B and Sharpe," Mechanical Testing of Polysilicon Thin Films with the ISDG" *Experimental Techniques*, v 21, n 2, Mar-Apr, 1997, p 32-35

[6] Haque, M.A and Saif, M.T.A , "Microscale Materials Testing Using MEMS Actuators" *Journal of Microelectromechanical Systems*, v 10, n 1, March 2001, p 146-52

[7] Z.Z Yuan, Q.X Dai, X.N. Cheng, K.M. Chen, L. Pen, A.D. Wang, " In situ SEM tensile test of high-nitrogen austenitic stainless steels" *Materials Characterization*, v 56, n 1, Jan. 2006, p 79-83

[8] Fan Li and Haibo Huang, "Analysis on the deformation and fracture behavior of carbon steel by in situ tensile test". *Journal of University of Science and Technology Beijing: Mineral Metallurgy Materials (Eng Ed)*, v 13, n 6, December, 2006, p 504-507

[9] E. Arzt "Size effects in materials due to microstructural and dimensional constraints: a comparative review". Acta Materialia, v 46, n 16, 9 Oct. 1998, p 5611-26

[10] Y. S. Kang and P.S. Ho, "Thickness dependent mechanical behavior of submicron aluminum films" *J, Electr. Mater*, Vol 26, no. 7, pp 805-813, 1997

[11] A.H. Chokshi, A. Rosen, J. Karch and H. Gleiter "On the validity of the Hall-petch relationship in nanocrystalline materials" Scripta Metallurgica, v 23, n 10, Oct. 1989, p 1679-84

[12] Misra A, Verdier M, Lu Y.C, Kung H,Mitchell T.E, Nastasi M and Embury J.D. "Structure and mechanical properties of Cu-X (X=Nb,Cr,Ni) nanolayered composites". Scripta Materialia, v 39, n 4-5, 4 Aug. 1998, p 555-60

[13] Carl V. Thompson and Roland Carel. " Stress and grain growth in thin films" . Journal of the Mechanics and Physics of Solids, v 44, n 5, May 1996, p 657-73

[14] J.S.C. Jang and C.C. Koch "The Hall-Petch relationship in nanocrystalline iron produced by ball milling". Scripta Metallurgica et Materialia, v 24, n 8, Aug. 1990, p 1599-604

[15] G.E. Fougere, J.R. Weertman, R.W. Siegel and S. Kim"Grain-size dependent hardening and softening of nanocrystalline Cu and Pd". Scripta Metallurgica et Materialia, v 26, n 12, 15 June 1992, p 1879-83

[16] K. Lu, W.D Wei and J.T. Wang." Microhardness and fracture properties of nanocrystalline Ni-P alloy". Scripta Metallurgica et Materialia, v 24, n 12, Dec, 1990, p 2319-2323.

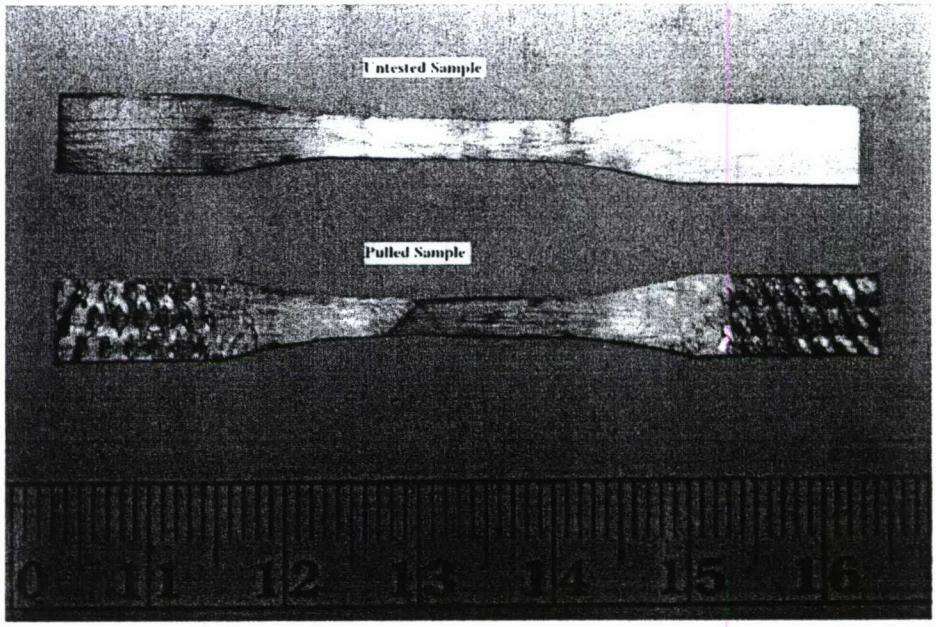

Fig 1. Ti-1100 large tensile samples. The upper one is the untested sample and the bottom one is the sample pulled at 0.5mm/min. The tensile elongation of the tested sample is 9.3 %.

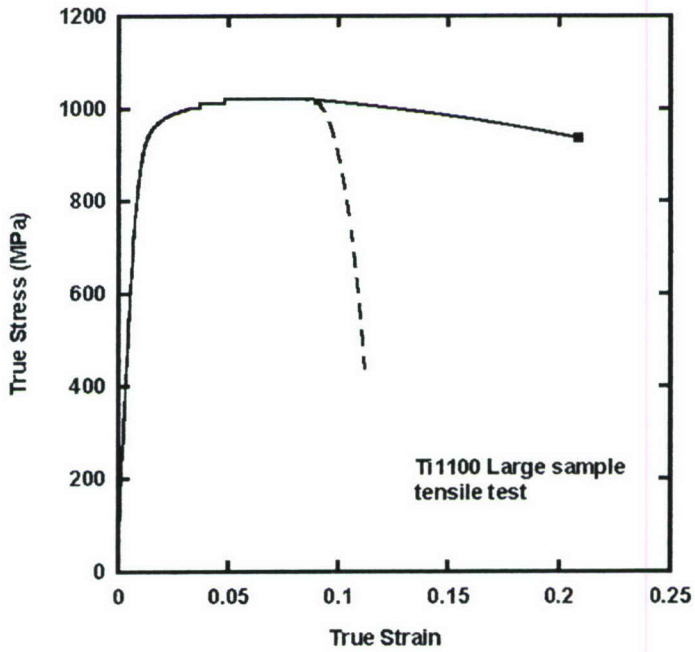

Fig 2. True Stress-Strain curve of the room temperature Ti-1100 sample pulled with strain rate of 0.5mm/min.The tensile strength is around 1000MPa.

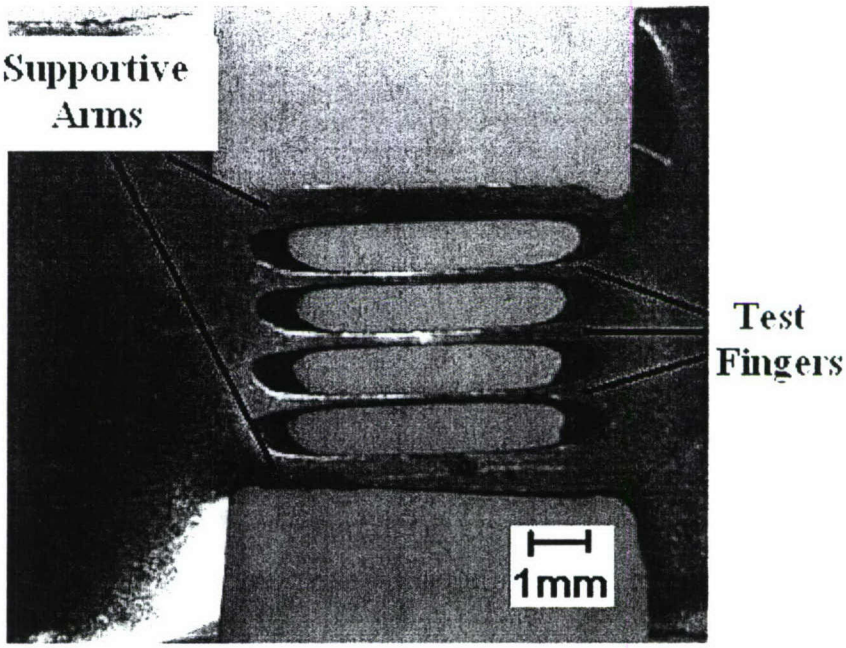

Fig 3. Photo of the multi-finger small sample.

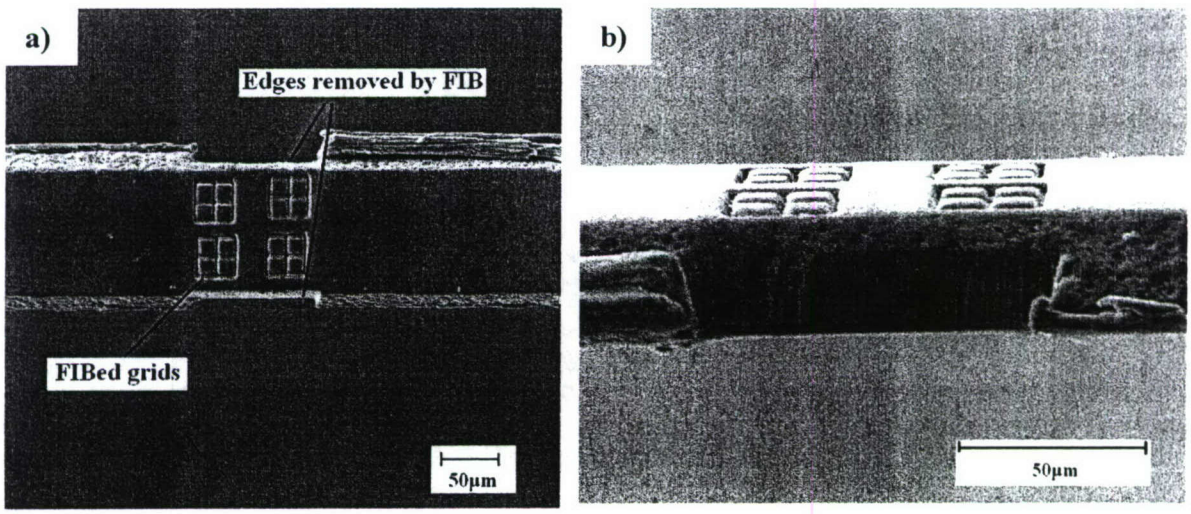

Fig 4 a) SEM photo taken from the top of the finger of the small sample.The recesses on each side of the finger were removed by the focused ion beam and the grids were also etched by the FIB with depth of 5µm 4b) Finger of the small sample 90 degrees from 4a, which showed a clean 100µm long FIB trimmed edge.

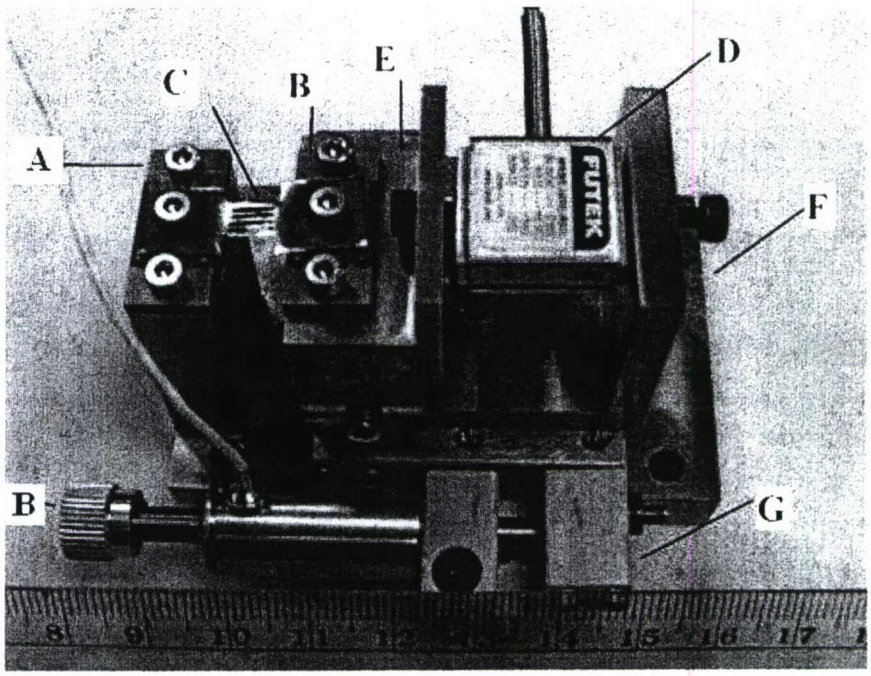

Fig 5. The small sample test apparatus. (A)Fixed crosshead (B) Mobile crosshead (C) small sample (D) Futek 5lbs loadcell (E) slide stage (F) Stainless steel frame (G) Loading flange (H) New Technology squiggle linear actuator.

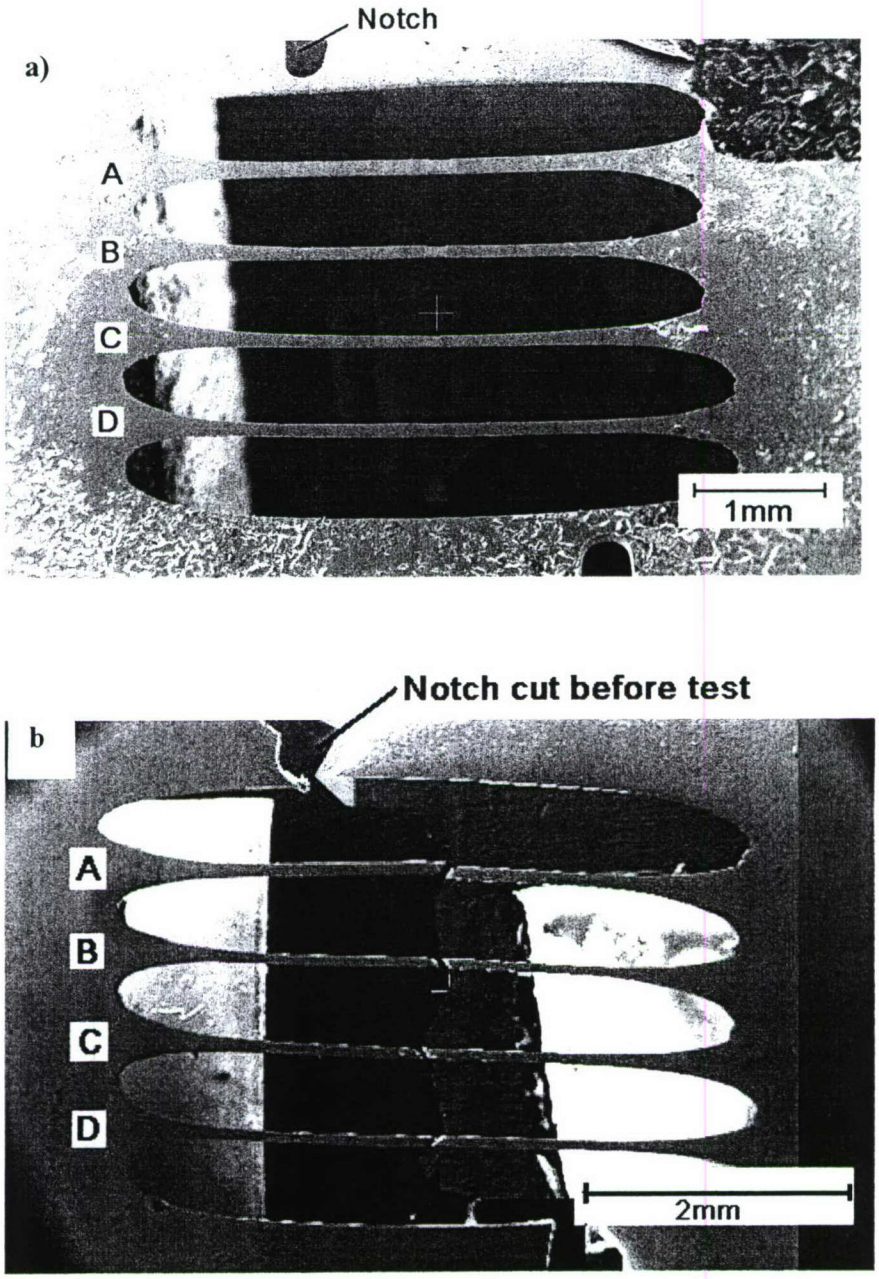

Fig 6. SEM photos of four-finger small sample before a) and after b) the tensile test

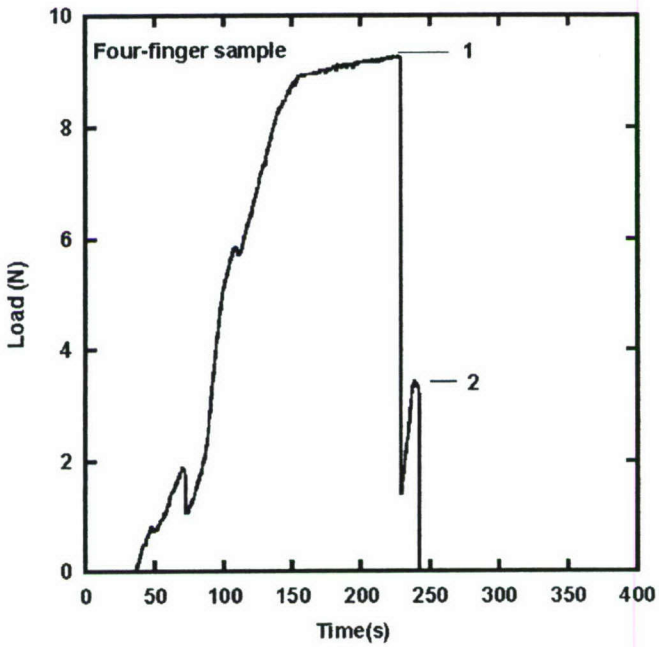

Fig 7. Load-Time curve of the four-finger sample.

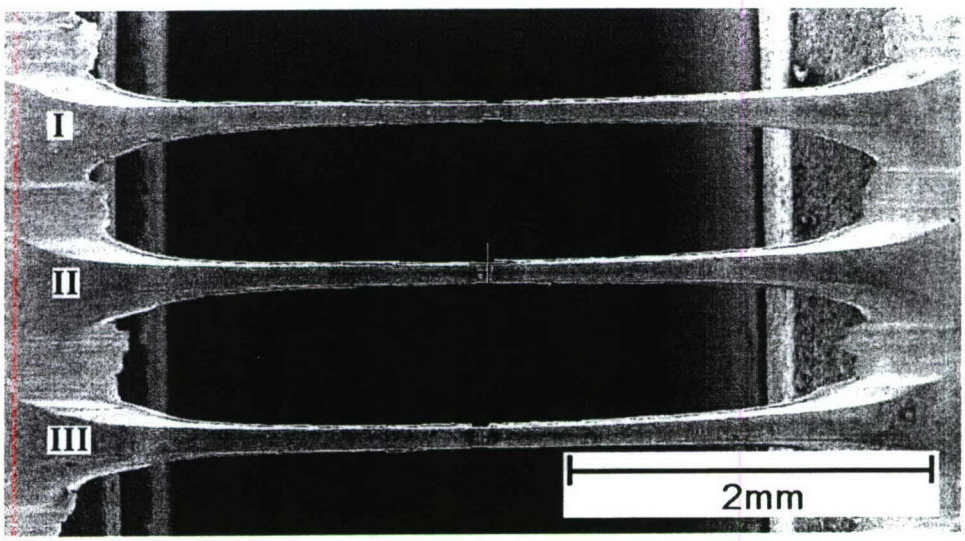

Fig 8. SEM photo of small sample 3 tested inside the SEM chamber.

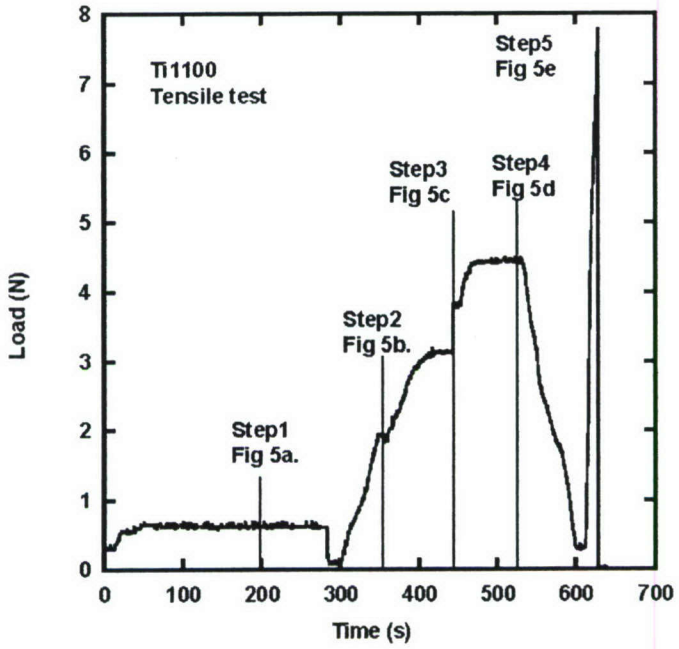

Fig 9. Load vs Time curve of the small sample tested inside the SEM chamber

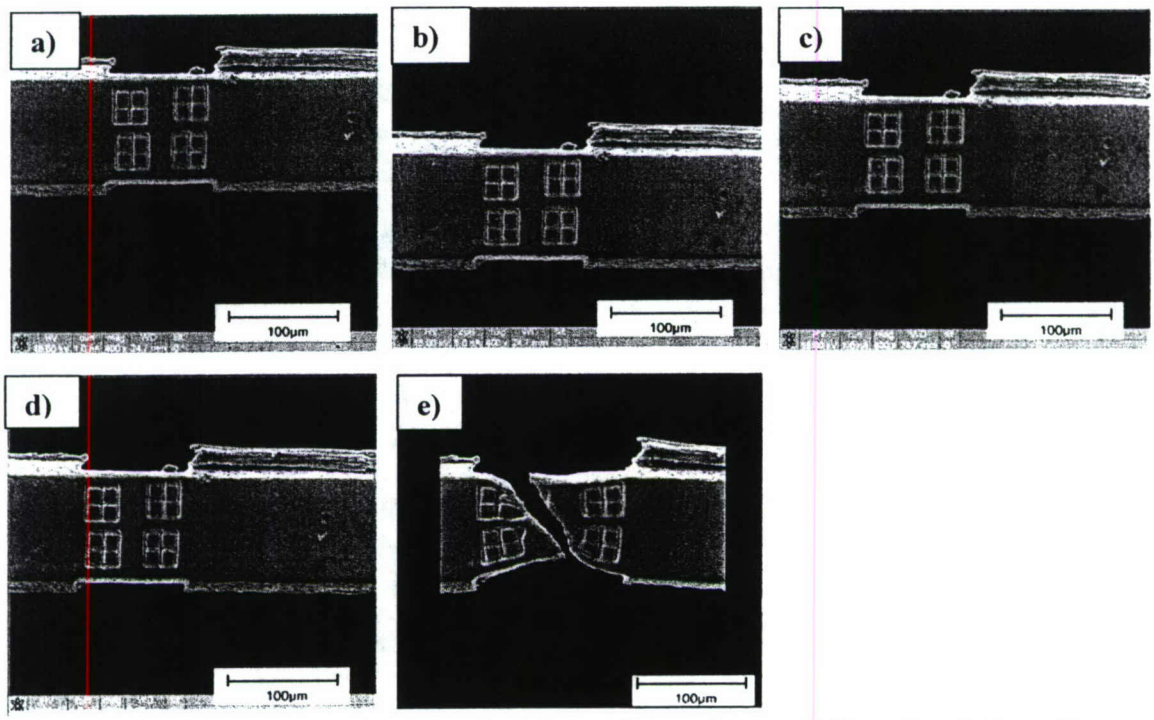

Fig 10. SEM photos taken by the end of a) step1 b)step2 c)step3 d)step4 and e) step5 of the small sample tensile test (sample 3) inside the SEM chamber.

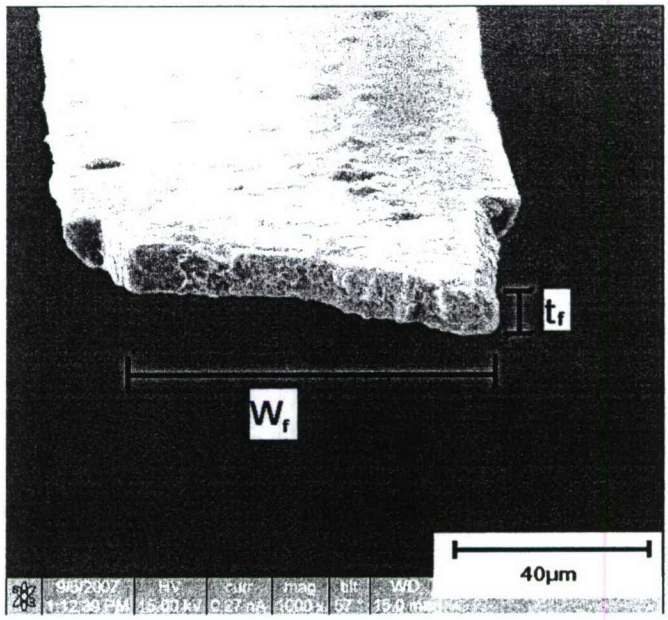

Fig 11. SEM photo of the fractured finger of the small sample. The final cross-section of the finger is w_f x t_f

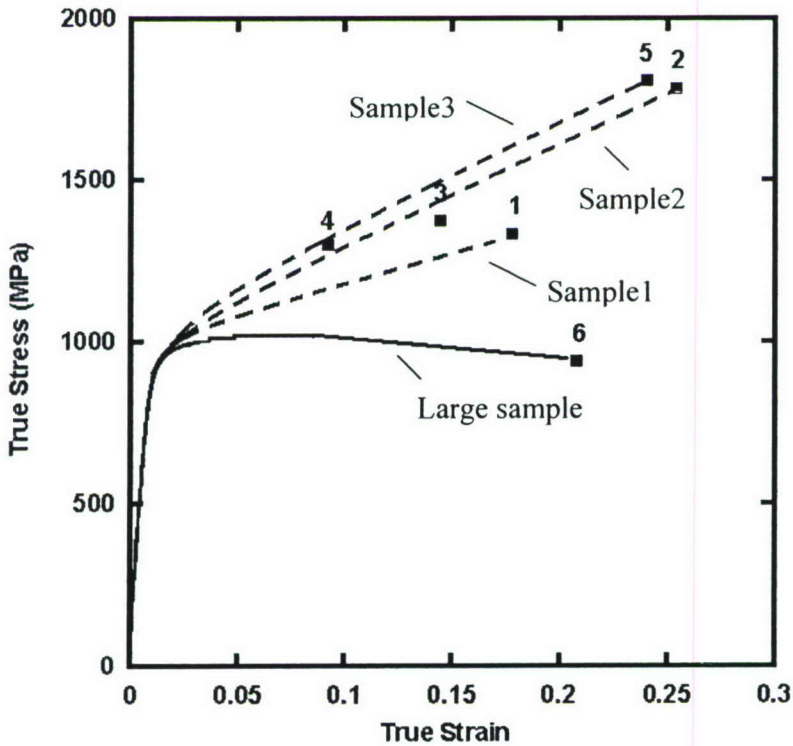

Fig 12. Extrapolated stress-strain curves of the small samples. The solid line is the stress-strain curve of the large sample.

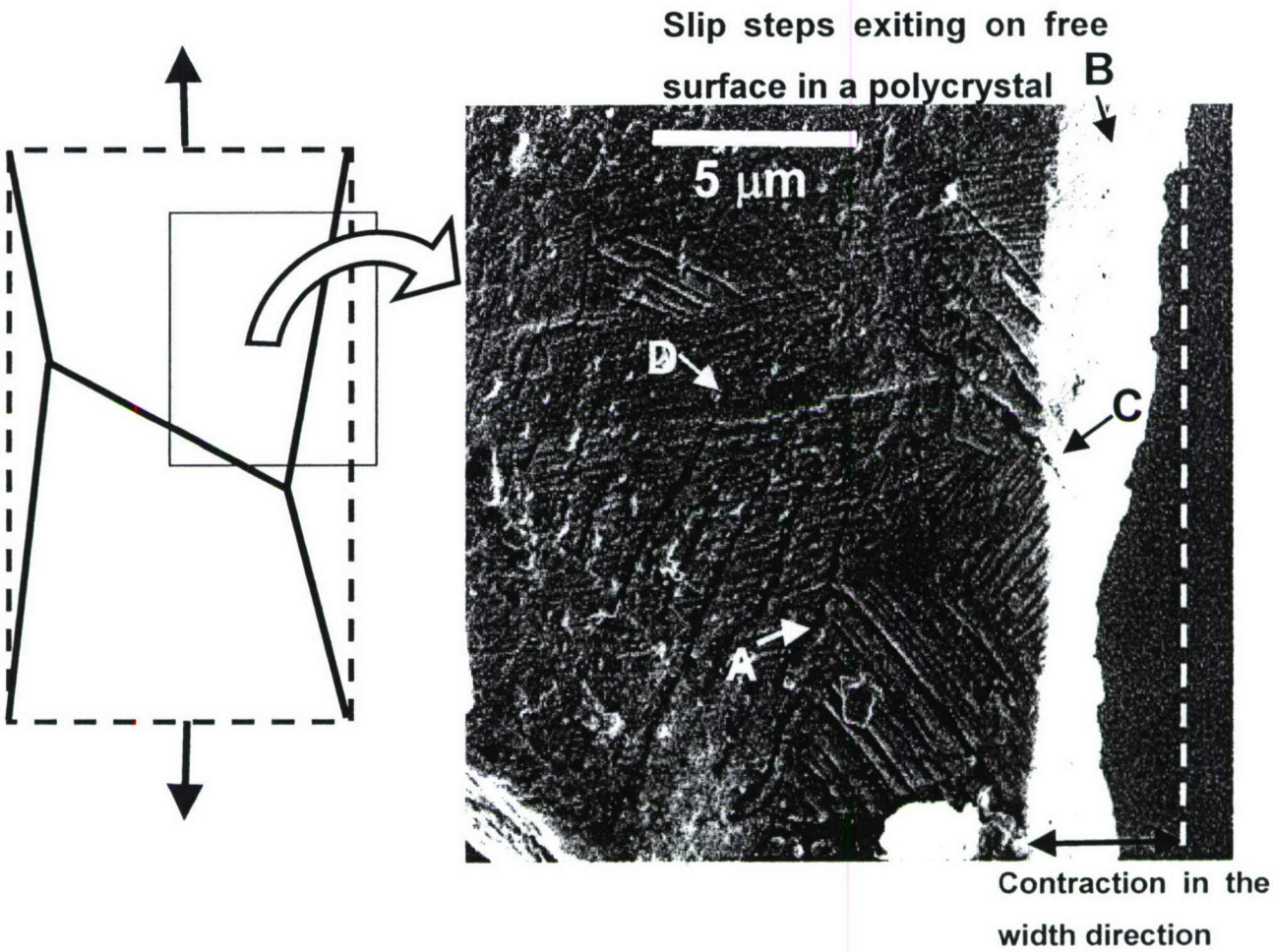

Fig. 13. A schematic and a microphotograph of polycrystalline micro-tensile specimen of titanium (25 μm x 25 μm) showing slip steps in several grains that eject on to free surfaces, front surface and side surface, arrows A, B, C; and also penetrate across grain boundary, arrow D. Contraction in the width direction indicate higher strain near bottom part of photo.